# Telomere-Driven Karyotypic Complexity Concurs with p16$^{INK4a}$ Inactivation in *TP53*-Competent Immortal Endothelial Cells

Victoria W. Wen,[1] Kaida Wu,[2] Sheik Baksh,[2] Rebecca A. Hinshelwood,[3] Richard B. Lock,[1] Susan J. Clark,[3] Malcolm A.S. Moore,[2] and Karen L. MacKenzie[1]

[1]Children's Cancer Institute Australia for Medical Research, Randwick, New South Wales, Australia; [2]Memorial-Sloan Kettering Cancer Center, New York, New York; and [3]Garvan Medical Research Institute, Darlinghurst, New South Wales, Australia

## Abstract

**Critically short telomeres promote chromosomal fusions, which in *TP53*-defective cells initiate the formation of cytogenetic aberrations that are typical of human cancer cells. Expression of the enzyme telomerase stabilizes normal and aberrant chromosomes by maintaining telomere length. However, previous investigations, including our own, have shown that overexpression of telomerase reverse transcriptase (hTERT) does not prevent net telomere shortening in human endothelial cells. In the present study, two mass cultures of hTERT-transduced bone marrow endothelial cells (BMhTERT) and 26 clones were employed to further investigate the immortalization process and consequences of telomere shortening. Eighty-five percent (22 of 26) of the clones and both mass cultures were immortalized. However, cytogenetic analyses revealed recurring cytogenetic aberrations in the mass cultures and 12 representative clones. Several of the recurring aberrations, including +5p, +11, −13, +19, and +20, and nonreciprocal translocations involving 17p and 2p were previously implicated in human carcinogenesis. One mass culture and a subset of clones (5 of 12) had complex karyotypes, characterized by cytogenetic heterogeneity and at least five chromosomal abnormalities. p16$^{INK4a}$ was silenced exclusively in the five clones and mass culture with complex karyotypes, whereas the p53/p21$^{cip1}$ pathway was defective in only one clone. Telomere dysfunction was implicated in the evolution of complex karyotypes by the presence of anaphase bridges, telomere associations, and dicentric chromosomes. These results show that complex karyotypes can evolve in *TP53*-competent cells and provide evidence that p16$^{INK4a}$ functions as a gatekeeper to prevent telomere-driven cytogenetic evolution. These investigations provide new insight to the role of p16$^{INK4a}$ as a tumor suppressor.** (Cancer Res 2006; 66(22): 10691-700)

## Introduction

The limited replicative life span of endothelial cells is largely attributed to the shortening of telomeres with each cell division (1). Telomeres are chromosomal-end structures that are composed of TTAGGG DNA repeats and folded into t-loops (2, 3). Telomeres function to protect against DNA degradation and prevent chromosomal fusions. However, critically short telomeres enable chromosome fusions, which contribute to the development of aneuploidy and chromosomal instability (4–6). Chromosome rearrangements resulting from telomere dysfunction drive progression of human malignancies (7–10). Excessive proliferation of endothelial cells is central to a number of premalignant and malignant disorders, including hemangioma, hemangioblastoma, and angiosarcoma (11). The molecular mechanisms underlying endothelial cell malignancies are not well defined, although a number of studies have shown complex karyotypes in angiosarcomas (12, 13).

In normal cells, telomere dysfunction and chromosomal abnormalities trigger *TP53*-mediated DNA damage signals that halt cell cycle progression and induce senescence (14–16). Inactivation of *TP53* circumvents DNA damage signals, enables continued proliferation of cells with dysfunctional telomeres, and thereby promotes chromosomal instability and transformation (5, 17). The cyclin-dependent kinase inhibitor p16$^{INK4a}$ is also up-regulated in senescent cells. Expression of p16$^{INK4a}$ inhibits phosphorylation of the retinoblastoma protein (pRB) and prevents cell cycle progression (18). A recent study indicated that up-regulation of p16$^{INK4a}$ in senescent cells may also be a consequence of telomere dysfunction (19).

Enforced expression of SV40 T antigens (SV40Tag) or the human papilloma virus *E6* and *E7* oncogenes, which inactivate pRB and *TP53* functions, extends the replicative life span of human endothelial cells (20, 21). However, telomeres in viral antigen–transformed cells continue to shorten, resulting in extensive chromosomal instability and eventual genetic catastrophe, which terminates the culture in a growth crisis (4). As a rare event, viral antigen–transformed cells escape crisis and are immortalized as a consequence of spontaneous activation of a telomere maintenance mechanism (4, 22).

The enzyme telomerase maintains telomeres in 80% to 90% of cancer cells (23). Ectopic expression of telomerase reverse transcriptase (hTERT) was shown to be sufficient to reconstitute telomerase enzyme activity and immortalize specific fibroblast and epithelial cell strains (24). However, inactivation of p16$^{INK4a}$ was implicated as a co-operating event in hTERT-mediated immortalization of other cell strains (25–30). Previous studies, including our own, showed that the life span of human endothelial cells was extended by overexpression of hTERT (31, 32). However, we found that two of three mass cultures of hTERT-transduced bone marrow endothelial cells (BMEC) underwent a growth crisis during immortalization (32). We concluded that telomerase was insufficient for immortalization and further showed that the combination of SV40Tag and hTERT very efficiently immortalized BMECs. Our results were consistent with investigations that showed mammary

**Note:** Supplementary data for this article are available at Cancer Research Online (http://cancerres.aacrjournals.org/).

Children's Cancer Institute Australia is affiliated with the University of New South Wales and Sydney Children's Hospital.

**Requests for reprints:** Karen MacKenzie, Children's Cancer Institute Australia for Medical Research, P.O. Box 81, High Street, Randwick, New South Wales, 2031 Australia. Phone: 61-2-9382-0048; Fax: 61-2-9382-1850; E-mail: k.mackenzie@unsw.edu.au.



doi:10.1158/0008-5472.CAN-06-0979

endothelial cells were immortalized by SV40Tag and hTERT, but not hTERT alone (33). In contrast, another report indicated that expression of hTERT was sufficient for immortalization of several other types of endothelial cells (31). These contrasting reports may partially reflect strain differences, as altered culture conditions did not reconcile our study with the latter (32). Despite the apparent differences, an important observation that was common to our study, and the latter was that telomeres continued to shorten in hTERT-transduced endothelial cells despite high levels of telomerase activity (31, 32).

Before the current investigation, the consequences of telomere shortening in hTERT-transduced endothelial cells have been unexplored. In the present study, we show that telomere shortening in hTERT-transduced BMECs results in chromosomal rearrangements, which mirror the types of aberrations found in human cancer cells, including angiosarcoma. Furthermore, complex karyotypes developed exclusively in a subset of cells that silenced $p16^{INK4a}$. These investigations show that reconstituted telomerase activity is not sufficient to prevent telomere dysfunction in human endothelial cells and are the first to show a relationship between $p16^{INK4a}$ inactivation and the development of karyotypic complexity in continuously proliferating *TP53*-competent cells.

## Materials and Methods

**Cell culture.** The establishment and propagation of hTERT-transduced BMEC mass cultures (BMhTERT-1 and BMhTERT-2) was previously described (32). BMhTERT clones were established by limiting dilution of the BMhTERT-1 mass culture at 28 population doublings in a 96-well plate. Wells containing a single cell were identified under an inverted microscope.

**Telomerase activity and telomere length measurements.** Telomerase activity was quantified using the telomeric repeat amplification protocol (TRAP), as previously described (32). The SK-N-SH neuroblastoma cell line (NB) was used as a positive control, and an internal control (TSNT) was included for quantitations. Telomerase activity was calculated as: $100 \times [(T - B) / TSNT] / [(NB - B) / TSNTNB]$, where $T$ is sample, $B$ is background, and TSNTNB is the internal control of the neuroblastoma. Mean telomere restriction fragment (TRF) length was measured using the TeloTAGGG telomere length assay kit (Roche, Indianapolis, IN) as previously described (30).

**Cytogenetics.** Cytogenetic analysis was done at Sydney Genetics, Sydney IVF (Sydney, Australia) using standard GTG banding techniques and examination of chromosomes at a resolution of 400 to 550 bands per haploid set. Chromosomal abnormalities were described according to the International System for Human Cytogenetic Nomenclature (1995).

**May Grunwald-Giemsa staining.** Cells ($1 \times 10^5$) were resuspended in 100 μL PBS, cytocentrifuged onto slides at $60 \times g$ for 5 minutes, then stained with May-Grunwald stain (BDH Laboratory Supplies, Poole, England) for 1 minute, rinsed in $H_2O$, immersed in 10% Giemsa stain for 12 minutes, and rinsed again in $H_2O$.

**Fluorescent *in situ* hybridization.** Fluorescence *in situ* hybridization (FISH) analysis was done at Sydney Genetics, Sydney IVF using probes for chromosome 17 centromere (CEP17 spectrum aqua, VYSIS, Downers Grove, IL), the *TP53* locus (LSI p53 spectrum orange, VYSIS) and the subtelomeric region of 17p (TelVysion 17p spectrum green, VYSIS). Images were digitally captured using CytoVision v2.7 software (Applied Imaging, Santa Clara, CA).

**Reverse transcription-PCR.** Total RNA was extracted using Trizol Reagent (Invitrogen, Carlsbad, CA) according to the manufacturer's instructions. First-strand cDNA was synthesized from 0.5 μg total RNA using 10 units M-MLV Reverse Transcriptase (Life Technologies, Gaithersburg, MD). The PCR reaction, including 100 ng cDNA, 2× SYBR Green PCR master mix (Applied Biosystems, Foster City, CA) and previously published primer sets for $p16^{INK4a}$ and $\beta_2$-microglobulin (34), was done on a ABI PRISM 7000 Sequence Detection System (Applied Biosystems) at 94°C for 10 minutes, then 40 cycles at 94°C for 30 seconds, 60°C for 30 seconds, and 72°C for 30 seconds, with a final step at 72°C for 10 minutes. PCR products were resolved through 1.5% agarose gels and visualized using Versadoc imaging system (Bio-Rad Laboratories, Hercules, CA).

**Immunoblot analysis.** Protein was isolated and immunoblot analysis done as previously described (30). Proteins were detected with the following antibodies: p53 (DO-1) monoclonal antibody (Santa Cruz Biotechnology, Santa Cruz, CA), pRB, $p16^{INK4a}$, and $p21^{Cip1}$ monoclonal antibodies (BD Biosciences PharMingen, San Diego, CA), and actin polyclonal antibody (Sigma, St. Louis, MO).

***CDKN2A* promoter methylation analysis.** The bisulfite reaction was carried out for 16 hours at 55°C on 2 μg of digested DNA, then semi-nested PCR amplifications were done as previously described (35, 36). PCR fragments were analyzed in 2× SYBR Green 1 Master mix using real-time PCR melting temperature dissociation, cycling through 95°C for 15 seconds, 60°C for 20 seconds, with the temperature increasing from 60°C to 90°C. CpGenome Universal Methylated Control DNA (Chemicon International, Temecula, CA) and Human Genomic DNA (Roche) were used as controls for fully methylated DNA and unmethylated DNA, respectively. Melting dissociation of the trace was analyzed on an ABI prism 7700HT Sequence Detection System. Results from dissociation curves were confirmed by direct sequencing and clonal sequencing of PCR products (35).

**Sequence analysis.** Genomic DNA was extracted by standard phenol/chloroform procedure and precipitated with 0.3 mol/L sodium acetate and 2 volumes of ethanol. Exons 2 to 11 of *TP53* gene were amplified by PCR using commercial primers from the Human p53 Amplimer Panel (Clontech, Palo Alto, CA) according to the manufacturer's protocol. PCR products were purified using BRESAspin PCR purification kit (GeneWorks, Adelaide, Australia) and sequenced by SUPAMAC (Camperdown, Australia).

## Results

**hTERT-transduced BMECs undergo crisis during immortalization.** BMhTERT-1 and BMhTERT-2 mass cultures were established by transduction of BMECs with a retroviral vector encoding hTERT (32). During immortalization, the BMhTERT-2 cell line underwent a prolonged growth crisis, whereas the BMhTERT-1 culture exhibited no clear crisis but had a reduced growth rate compared with early passage cells. For the present investigations, 32 clones were established by limiting dilution of the BMhTERT-1 mass culture at 28 population doublings (Fig. 1*A*). Out of 32 clones, 26 had an extended life span compared with parental BMEC cultures, which senesced at ~35 population doublings. Twenty of these 26 clones underwent a growth crisis, characterized by an overall decrease in proliferation, increased cell death, the appearance of cells with a senescent morphology, and demonstrable senescence-associated β-galactosidase activity (data not shown). The onset of crisis occurred at ~50 population doublings. The duration of crisis varied, lasting up to 200 days for some clones. Most clones (16 of 20) eventually escaped crisis and resumed proliferation. Overall, 22 of 26 (85%) of the BMhTERT clones that bypassed senescence proliferated beyond 100 population doublings (~3-fold increase in life span) and were considered immortalized. These results confirm that BMECs undergo a crisis during immortalization and show that crisis may be masked in mass cultures by clonal heterogeneity.

**Crisis was independent of telomere length and the level of telomerase activity.** To determine whether crisis was triggered by short telomeres, the mean telomere length of BMhTERT clones was measured at multiple time points (Fig. 1*B* and *C*). The mean telomere length of BMhTERT-1 mass cultured cells declined from 8.5 kbp (38 population doublings) at a rate of 67 bp/population doubling, until it stabilized around 3.4 kbp (115-130 population doublings; Fig. 1*C*). These results were striking considering we previously found that parental BMECs senesced with an average

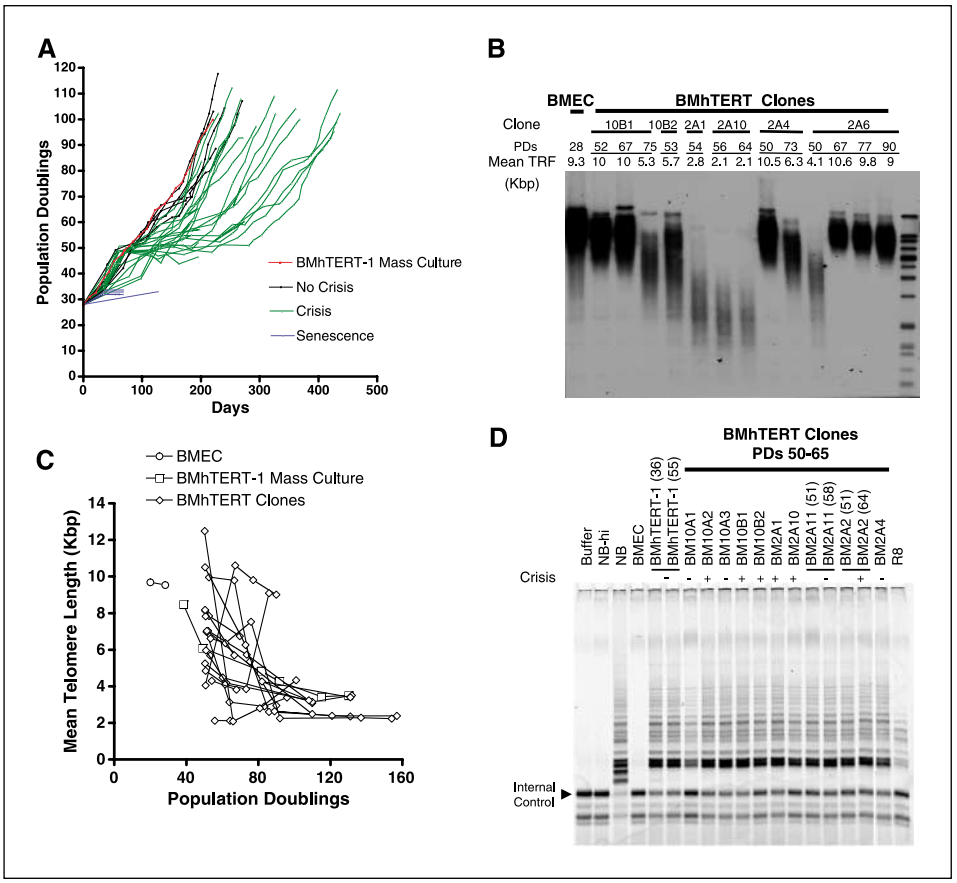


**Figure 1.** Proliferation, telomere length, and telomerase enzyme activity in BMhTERT cells. *A,* proliferation of BMhTERT-1 mass culture (*red*) and derivative clones. *Blue line,* clones that underwent senescence; *green line,* clones that underwent crisis; *black lines,* clones that exhibited no clear crisis. *B,* representative TRF of BMhTERT clones. Mean telomere length of each cell line is indicated above the gel. *C,* graphical representation of changes in the mean telomere length of BMhTERT cells during immortalization. *D,* a representative TRAP gel of the BMhTERT clones during crisis [50-65 population doublings (*PD*)]. *NB,* SK-N-SH neuroblastoma cell line (positive control); *NB-hi,* heat-inactivated lysate from SK-N-SH neuroblastoma cell line (negative control); *R8,* template DNA (positive control).

telomere length of 6.0 kbp (32). Consistent with the mass culture, the mean telomere length of most clones eventually stabilized around 3.0 kbp (between 3.6 and 2.4 kbp; Fig. 1*C*). Indeed, clones BM2A11 and BM2A9 maintained telomere length in this range until at least 179 and 281 population doublings, respectively (additional data not shown). The apparent shortening of mean telomere length at earlier population doublings (<85) and eventual maintenance at a subsenescent length were likely a reflection of preferential maintenance of critically short telomeres (37, 38).

At the onset of crisis (around 50 population doublings), the telomere length of different BMhTERT clones ranged from 12.5 to 2.1 kbp (Fig. 1*C*). However, there was no significant difference in the average telomere length of clones that went into crisis (7.6 $\pm$ 0.7 kbp, $n$ = 6) compared with clones that showed no distinct crisis (7.7 $\pm$ 0.8 kbp, $n$ = 9; Student's $t$ test, $P$ = 0.8925). Furthermore, the average telomere length was significantly shorter at late passage (4.9 $\pm$ 0.7 kbp, $n$ = 14, at >65 population doublings) compared with earlier time points (7.7 $\pm$ 0.5 kbp, $n$ = 15 at <65 population doublings; Student's $t$ test, $P$ = 0.006). These results are consistent with the decline in mean telomere length observed in the mass culture but are converse to the results expected if crisis was due to telomere shortening. To investigate whether shortening of mean telomere length or crisis was due to low levels of telomerase activity, the TRAP assay was done on representative clones (Fig. 1*D*; additional data not shown). Quantitation of telomerase activity against an internal control and tumor cell line revealed no significant difference in telomerase activity assayed at pre- and post-crisis time points (25.2 $\pm$ 4.4, $n$ = 13 compared with 27.1 $\pm$ 3.8, $n$ = 9, respectively; Student's $t$ test, $P$ = 0.75). Regression analysis showed no significant correlation between the level of telomerase activity and mean telomere length of BMhTERT clones at crisis ($n$ = 17, $r^2$ = 0.03, $P$ = 0.53). Overall, results from TRF and TRAP analyses showed that (*a*) telomeres were maintained at a subsenescent average telomere length; (*b*) crisis was independent of the mean telomere length and the level of telomerase activity; and (*c*) shortening of mean telomere length in BMhTERT clones was not due to low levels of telomerase activity.

**Telomere dysfunction leads to the evolution of cytogenetic abnormalities.** Karyotypic analyses were done to investigate potential telomere dysfunction in BMhTERTs. No cytogenetic abnormalities were detected in the parental BMECs and the BMhTERT-1 mass culture at early passage (35 population doublings; Table 1). However, an additional copy of chromosome 11 (+11) was detected in BMhTERT-1 at 65 population doublings and persisted until at least 135 population doublings. No other abnormalities were detected in this mass culture, despite telomere shortening to 3.5 kbp at 135 population doublings. Trisomy 11 was also detected in 9 of 12 BMhTERT clones (Table 1). It is important to note that the clones were established from the BMhTERT-1 mass culture at 28 population doublings, which was before the appearance of +11 in the mass culture. Other recurring cytogenetic abnormalities that were present in three or more cell lines included −Y, del(1)(q12), i(5)(p10), +5, −13, add(13)(p11.2), t(2;17)(p13;p13.3), +19, add(19)(q13.1), +20, and −21. There were also various abnormalities affecting chromosome arm 2p in four clones. To determine whether the recurring abnormalities were present at a low frequency in the mass culture at the time of cloning, an additional 400 BMhTERT-1 cells at 33 population

**Table 1.** Summary of cytogenetic analysis, telomere length, and crisis in BMhTERT clones and mass cultures

| Cell line | Population doublings* | Mean telomere length † | Karyotype | Crisis ‡ |
|---|---|---|---|---|
| BMEC | 31 | ND | 46, XY, no abnormalities [20] | NA |
| BMhTERT-1 mass culture | 35 | 8.5 | 46, XY, no abnormalities [20] | NA |
| | 65 | 5.5 | 47, XY, +11 [20] | NO |
| | 84 | 4.5 | 47, XY, +11 [20] | NO |
| | 113 | 4.0 | 47, XY, +11 [100] | NO |
| | 135 | 3.5 | 47, XY, +11 [20] | NO |
| BMhTERT clones | | | | |
| BM2A7 | 111 | 3.1 | 47, XY, +11 [27] | YES |
| BM2A11 | 107 | 2.5 | 47, XY, +11 [20] | NO |
| BM2B2 | 105 | 9.0 | 47, XY, +11 [20] | NO |
| BM2A6 | 84 | 8.5 | 45, X, −Y, +11, −13 [19] | YES |
| BM2A10 | 98 | ND | 48, XY, +11, +19 [21] | YES |
| BM2A2 | 82 | 2.5 | 47, XY, +11, del(9)(p22p24) [20] | YES |
| BM2A2 | 109 | ND | 47, XY, +11, del(9)(p22p24) [24] | YES |
| BM10A3 | 109 | 3.0 | 45, XY, add(9)(p13), −13 [20] | NO |
| BM2A9 | 92 | 2.3 | 48, X, −Y, add(2)(p13), +11, add(13)(p11.2), t(2;17)(p13;p13.3), +19, add(19)(q13.1), +20 [13]/48, idem, −add(13), hsr(13)(p11.2) [6] | YES |
| BM10B1 | 75 | 5.4 | 45, XY, inv(2)(p?13q35), −13 [21] | YES |
| BM10B1 | 108 | 3.0 | 48, XY, der(2)t(2;13)(p11.2;q12), +5, i(5)(p10), −13, add(15)(p11.2), t(2;17)(p13;p13.3), +19, +20 [320] | YES |
| BM10B1 | 164 | ND | 47-49, XY, der(2)t(2;13)(p11.2;q12), +5, i(5)(p10), −13, add(15)(p11.2), t(2;17)(p13;p13.3), +19, +20 [9]/48, XY, idem, add(18)(q32), +19, +20 [7]/47, idem, add(19)(p11.2), −20 [4] | YES |
| BM2B8 | 81 | 2.8 | 45-47, X, −Y, add(2)(p13), +11, add(13)(p11.2), t(2;17)(p13;p13.3), +19, add(19)(q13.1), +20, −21 [14]/83-94, XX, −Y, −Y, del(1)(q12), add(2)(p13)x2, add(12)(q24.3)x2, t(2;17)(p13;p13.3)x2, +19, +19, add(19)(q13.1)x2, +20 [5] | YES |
| BM2B8 | 109 | 4.0 | 46-49, XY, +5, i(5)(p10), −13, t(2;17)(p13;p13.3), +19, +20, add(22)(p11.2) [12]/46-49, X, −Y, add(2)(p13), +11, add(13)(p11.2), t(2;17)(p13;p13.3), +19, add(19)(q13.1), +20, −21 [31]/87-90, XX, −Y, −Y, del(1)(q12), add(2)(13)x2, i(5)(p10), −6, add(12)(q24.3)x2, −13,−13, t(2;17)(p13;p13.3)x2, +19, add(19)(q13.1), +20 [14]/87-91, idem, −i(5)(p10), t(2;17)(p13;p13.3), +20 [43] | YES |
| BM2B12 | 108 | 3.0 | 45-47, X, −Y, add(2)(p13), +11, add(13)(p11.2), t(2;17)(p13;p13.3), +20, −21 [8]/76-92, XX, −Y, −Y, add(1)(q12), del(1)(q12), −2, add(2)(p13)x2, −4, −5, −6, −8, −9, −10, +11, add(12)(q24.3)x2, −13, −13, add(13)(p11.2)x2, −15, −16, −17, t(2;17)(p13;p13.3)x2, +19, add(19)(q13.1), +20, +20, +22 [12] | YES |
| BM2A4 | 103 | 2.6 | 74-78, XX, −Y, +1, add(1)(q12), +2, del(2)(p21p25)x2, −3, −3, −4, −4, +5, i(5)(p10), +6, +7, +8, −9, del(9)(p22p24), +11, add(11)(q24), +12, −13, +14, +15, add(15)(p11.2)x2, +16, der(17)t(3;17)(q10;p10)x2, +18, +19, +20, −21, +2mars [10]/119-145, XXXX, −Y, −Y, add(1)(q12), del(1)(q12), −2, −3, −3, −4, −4, +5, i(5)(p10), +6, +6, +6, +7, +7, −9, −9, del(9)(p22p24)x2, +11, +11, −12, −12, +12, −13, −13, +14, add(15)(p11.2)x2, der(15)t(8;15)(q10;q10), +17, der(17)t(3;17)(q10;p10)x2, add(17)(p10)x2, +18, +18, +19, +20, −21, −21, −21, −21, +22, +22, +3mars [20] | NO |
| BMhTERT-2 mass culture | 90 | 2.5 | 49, XY, +5, i(5)(p10), −13, t(2,17)(p13;p13.3), +19, +20, +20, [15]/46, XY [4] | YES |

NOTE: Numbers in square brackets indicate the number of cells analyzed.
Abbreviations: idem, as mentioned previously; mars, marker chromosomes; ND, not determined; NA, not applicable.
*Population doublings at the time cytogenetic analysis was done.
†Mean telomere length in kbp as determined by TRF analysis around the time cytogenetic analysis was done.
‡Indicates whether or not a clone underwent a clear crisis defined as a period of slowed growth.

doublings were scored for aberrations involving the chromosomes most frequently affected (i.e., chromosomes 2, 11, 13, 17, 19, 21, and 22). No abnormalities of these chromosomes were detected in 400 metaphases.

The mass cultures and clones could be clearly subgrouped according to karyotypic complexity. Simple karyotypes, defined as near diploid with only one to two abnormalities, were detected in 7 of 12 clones and the BMhTERT-1 mass culture. In contrast, the remainder of the clones (5 of 12) and the BMhTERT-2 mass culture had complex karyotypes, characterized by at least five chromosomal abnormalities and frequent polyploidy. The detection of cytogenetically related sublines within clones with complex karyotypes were indicative of karyotypic evolution. BM2A4 had the most complex karyotype and exhibited overt chromosomal instability, characterized by a high frequency of random aberrations and numerous non-clonal marker chromosomes. Cells with simple verses complex karyotypes could not be distinguished based on proliferative rate or whether they went through crisis. Telomere length dynamics also did not predict karyotypic status. For instance, both BM2A7 (simple karyotype) and BM2B12 (complex karyotype) had a mean telomere length of about 5.0 kbp at 50 population doublings and showed shortening to around 3 kbp by ~110 population doublings.

Short dysfunctional telomeres promote chromosomal aberrations via breakage-fusion-bridge (BFB) cycles, which are initiated by the fusion of sister chromatids that have lost telomeres. BFB events promote specific patterns of chromosome abnormalities, including nonreciprocal translocations, deletions, amplifications, and whole chromosome losses (5, 8, 39). The possible involvement of BFB events in karyotypic evolution of BMhTERTs was investigated by screening for dicentric chromosomes, telomere associations, and ring chromosomes, which are the hallmarks of telomere dysfunction and BFB cycles. In BM2B8, which had a complex karyotype with two evolving sublines, 12 of 155 G-banded metaphase cells harbored dicentric chromosomes (5 cells) or telomere associations (7 cells; Fig. 2*A*). Six of 12 of these telomere associations and dicentrics involved chromosome arms that were detected in clonal rearrangements in this cell line at a later time point (additional data not shown). In the BM2A4 cell line, 12 of 20 (60%) cells showed evidence of BFB events, including ring chromosomes, telomere associations, and anaphase bridges. Multipolar mitoses and lagging chromatin, which are associated with a high rate of anaphase bridging, were also detected in BM2A4 (Fig. 2*B*). In contrast, no BFB events were detected in BMhTERT-1 (100 cells scored), which exhibited a simple karyotype and no evidence of heterogeneity or evolution. The nonreciprocal translocations and chromosome losses detected in BMhTERTs are consistent with BFB-generated karyotypic changes (39). Taken together, these data indicate telomere dysfunction and BFB events drove the evolution of karyotypic complexity in BMhTERT cells.

**Loss of the subtelomeric region of chromosome arm 17p in all complex karyotypes.** The nonreciprocal translocation t(2;17)(p13;p13.3), which involved translocation of the entire short arm of chromosome 2 to 17p13.3, was detected in the BMhTERT-2 mass culture and four of five clones with complex karyotypes. BM2A4, which also had a complex karyotype, did not have t(2;17)(p13;p13.3) but had alternative rearrangements of 17p [der(17)t(3;17)(q10;p10) × 2 and add(17)(p10) × 2] that resulted in loss of the entire 17p arm. Because the *TP53* gene is located on 17p, FISH analysis was done for *TP53*, as well as 17p subtelomeric sequence and chromosome 17 centromere in BM2A4 and BM2B8

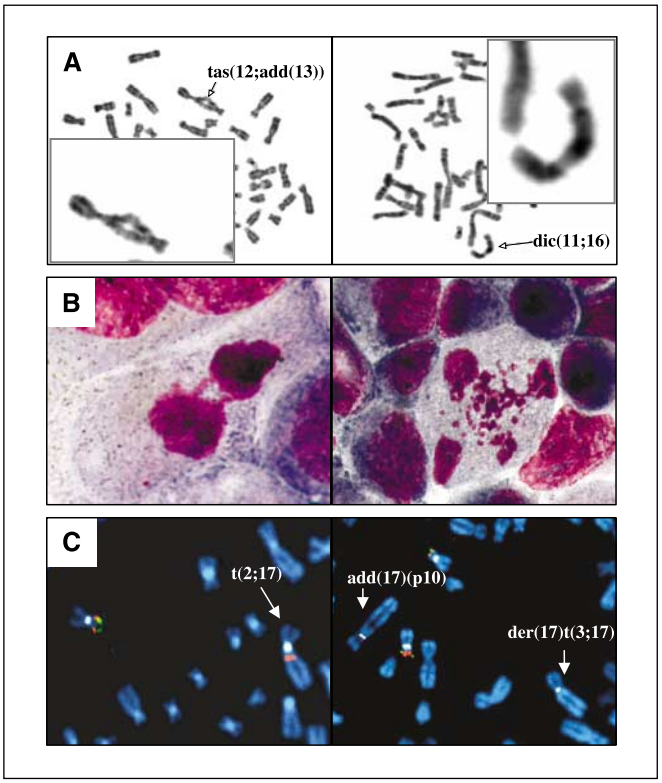


**Figure 2.** Evidence of BFB cycle in BMhTERT clones with complex karyotypes. *A, left,* telomere association (*tas*); *right,* dicentric chromosome (*dic*) in BM2B8. *B, left,* anaphase bridge; *right,* multipolarity in BM2A4. *C,* FISH analysis. *Left,* BM2B8 with t(2;17)(p13;p13.3); *right,* BM2A4 with add(17)(p10) and der(17)t(3;17)(q10;p10). *Green,* subtelomere; *red, TP53* locus; *white,* 17 centromere.

[an example of a cell line with t(2;17)(p13;p13.3); Fig. 2*C*]. The results showed that all rearranged 17p arms in both cell lines had lost subtelomeric DNA, whereas the *TP53* locus was retained on all copies of chromosome 17 in the BM2B8 cells, including chromosomes with the t(2;17)(p13;p13.3) rearrangement. Although *TP53* was also retained on two apparently normal copies of chromosome 17 in BM2A4, it was deleted from chromosomes with der(17)t(3;17)(q10,p10) and add(17)(p10). Thus, whereas loss of 17p subtelomeric sequence was common to all clones with complex karyotypes, the *TP53* locus was only lost in association with der(17)t(3;17)(q10;p10) and add(17)(p10), which only occurred in BM2A4.

**Repression of p16$^{INK4a}$ by methylation occurs in a subset of clones.** Immunoblot analysis of p16$^{INK4a}$ showed readily detectable protein in the BMhTERT-1 mass culture at late passage (131 population doublings), as well as in BM2A7, BM2A11, BM2B2, BM2A6, BM2A10, BM2A2, and BM10A3 at post-crisis time points (Fig. 3*A*). In contrast, p16$^{INK4a}$ was undetectable in the post-crisis BMhTERT-2 mass culture and BM2A9, BM2B8, BM2B12, and BM2A4 clones. Down-regulation of p16$^{INK4a}$ in the latter cell lines seemed to be complete, as there was no mRNA detected by real-time PCR comparison of these cell lines with the MCF-7 cell line, which has a homozygous deletion of the *CDKN2A* locus (Fig. 3*B*; additional data not shown). p16$^{INK4a}$ protein was detected at a very low level in BM10B1 at 107 population doublings (Fig. 3*A*), whereas real-time PCR analysis of clone BM10B1 revealed robust mRNA expression at 87 population doublings but no detectable p16$^{INK4a}$

mRNA by 112 population doublings (Fig. 3*B*). Notably, the timing of $p16^{INK4a}$ repression in BM10B1 at about 107 population doublings did not correspond with the main growth crisis, which began at 52 population doublings in this cell line. Overall, $p16^{INK4a}$ protein expression was repressed in 5 of 12 post-crisis clones.

We investigated the possibility that $p16^{INK4a}$ was silenced by methylation of *CDKN2A* CpG island promoter regions by performing bisulfite methylation followed by PCR amplification (36). Analysis of the heat dissociation curves of the PCR products, as well as direct and clonal PCR sequence analysis showed a direct correlation between promoter hypermethylation and $p16^{INK4a}$ silencing (Fig. 3*C*; Supplementary 1; Table 2). For example, *CDKN2A* promoter was methylated and inactivated in clones BM2A9, BM2B8, and BM2B12, as well as BMhTERT-2 mass culture at late passage. Furthermore, the *CDKN2A* promoter was methylated in BM10B1 at 115 population doublings, but not 90 or 75 population doublings, which is consistent with expression data (Fig. 3*A* and *B*; Supplementary 1; Table 2). Hypermethylation is, therefore, the likely cause for gene silencing in the BMhTERT-2 mass culture and in four of five clones. The *CDKN2A* promoter sequence could not be amplified from clone BM2A4, which suggests that $p16^{INK4a}$ expression was silenced in this cell line by gene deletion or rearrangement. Overall, these data show that $p16^{INK4a}$ expression was extinguished before 120 population doublings in 5 of 12 BMhTERT clones and one of two mass cultures. Further, inactivation of $p16^{INK4a}$ may occur but is not essential for hTERT-mediated immortalization of BMECs.

When the clones were grouped according to karyotypic complexity, it was striking that $p16^{INK4a}$ expression was repressed exclusively in the five clones and one mass culture that had complex karyotypes (Table 2). The relationship between $p16^{INK4a}$ repression and karyotypic complexity was highlighted by the time course of BM10B1 (Fig. 3; Tables 1 and 2). This clone expressed $p16^{INK4a}$ and had a simple karyotype at 75 population doublings, then developed a complex karyotype at 108 population doublings when $p16^{INK4a}$ was down-regulated and showed clonal heterogeneity by 164 population doublings. These data provide evidence that inactivation of $p16^{INK4a}$ permits accumulation of cytogenetic aberrations, and, conversely, that $p16^{INK4a}$ functions as a gatekeeper to prevent karyotypic evolution.

**Dysfunction of pRB phosphorylation in a subset of post-crisis clones.** To investigate whether repression of $p16^{INK4a}$ affected pRB function, immunoblot analysis of phosphorylated and hypophosphorylated pRB was done on BMhTERTs treated with 25 μmol/L of the DNA damage agent etoposide (VP-16; Fig. 4*A*). As expected, pRB was detected in untreated parental BMECs as a broad band, representing both phosphorylated and hypophosphorylated forms, and was down-regulated and detected as a single low molecular weight band, representing the hypophosphorylated form, in VP-16-treated BMECs. The same normal response to VP16 treatment was observed in four pre-crisis cultures (BMhTERT-2, BMhTERT-1, BM2A2, and BM2A10), as well as all post-crisis clones that retained $p16^{INK4a}$ expression. Among the five clones and one mass culture that silenced $p16^{INK4a}$, two clones (BM2A9 and BM10B1) and the mass culture (BMhTERT-2) also showed a normal pRB response, whereas pRB remained up-regulated and phosphorylated following treatment of BM2B8, BM2B12, and BM2A4, which were also $p16^{INK4a}$ negative. BM10B1 at 101 population doubling showed a weak response, which was consistent with incomplete down-regulation of $p16^{INK4a}$ at this time point. Overall, the data show that dysfunction of pRB phosphorylation corresponded with inactivation of $p16^{INK4a}$ in some but not all BMhTERT cultures. Notably, the three clones that exhibited pRB dysfunction all developed polyploid sublines (Table 1). In contrast, the three cell lines that were $p16^{INK4a}$ negative but retained normal pRB function were near diploid at the time of the assay.

**Loss of *TP53* function is infrequent during immortalization of BMhTERT cells.** The *TP53* DNA damage response was investigated by treating cells with VP-16, then assessing expression of p53 and its transcriptional target $p21^{Cip1}$ by immunoblot analysis (Fig. 4*B*). In the parental BMECs, expression of p53

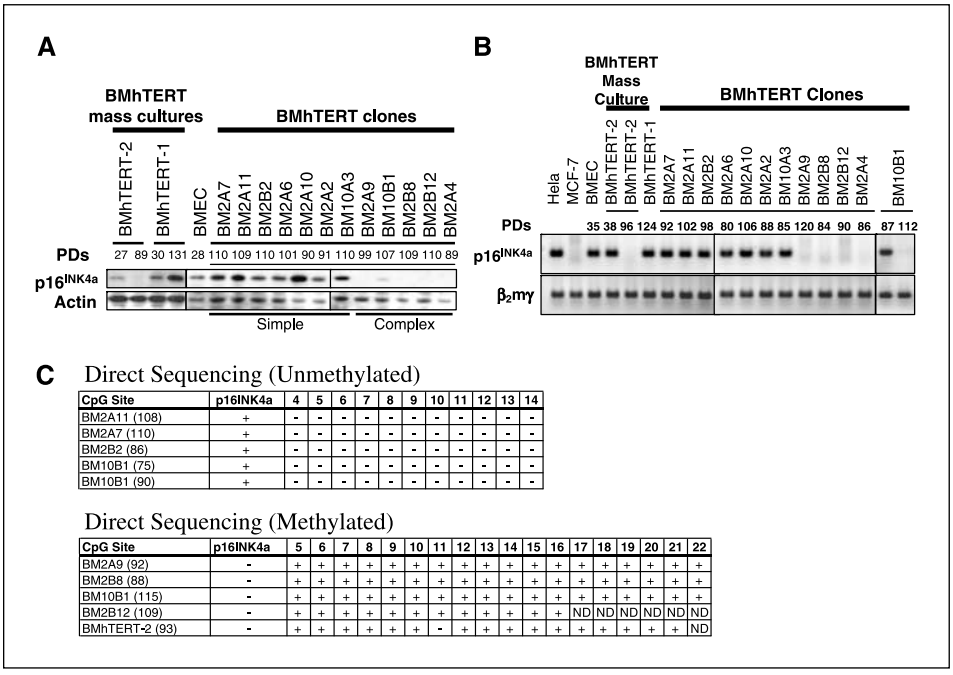


**Figure 3.** Expression of $p16^{INK4a}$ protein and mRNA in BMhTERTs. *A,* immunoblot analysis of $p16^{INK4a}$ protein. Actin was used as a loading control. *B,* reverse transcription-PCR products, $p16^{INK4a}$ (150 bp), and $\beta_2$-microglobulin (150 bp) (control), run on an agarose gel. HeLa and MCF-7 mRNAs were used as positive and negative controls, respectively. *C,* direct sequencing profile of CpG sites 4 to 22. $p16^{INK4a}$ expression, determined by immunoblot and/or reverse transcription-PCR, is indicated. *ND,* uninterpretable results. Numbers in brackets are population doublings at the time of the assay.

**Table 2.** Repression of p16$^{INK4a}$ exclusively in cells with complex karyotypes

| Cell line | p16$^{INK4a}$ status | | | | p53 function* | pRB/regulation † | Karyotype ‡ |
|---|---|---|---|---|---|---|---|
| | Expression§ | | Methylation‖ | | | | |
| | Protein | mRNA | Melting temperature | Direct sequencing | | | |
| BMEC | + (28) | + (35) | ND | ND | + (28) | + (28) | Normal (31) |
| BMhTERT-1 mass culture | + (30) | ND | ND | ND | + (37) | + (37) | Normal (35) |
| | + (41) | ND | ND | ND | ND | ND | Simple (65) |
| | + (61) | ND | ND | ND | ND | ND | Simple (84) |
| | + (100) | ND | ND | ND | + (110) | + (110) | Simple (113) |
| | + (131) | + (124) | − (135) | ND | ND | ND | Simple (135) |
| BMhTERT clones | | | | | | | |
| BM2A7 | + (112) | + (92) | − (110) | − (110) | + (112) | + (112) | Simple (111) |
| BM2A11 | + (84) | + (102) | − (108) | − (108) | + (84) | + (84) | Simple (107) |
| BM2B2 | + (110) | + (98) | − (86) | − (86) | + (110) | + (110) | Simple (105) |
| BM2A6 | + (104) | + (80) | − (82) | ND | + (104) | + (104) | Simple (84) |
| BM2A10 | + (95) | + (106) | − (117) | ND | + (92) | + (92) | Simple (98) |
| BM2A2 | + (120) | + (88) | − (83) | ND | + (91) | + (91) | Simple (109) |
| BM10A3 | + (112) | + (85) | − (110) | ND | + (110) | + (110) | Simple (109) |
| BM10B1 | ND | + (87) | − (75) | − (75) | ND | ND | Simple (75) |
| BM10B1 | +/− (107) | − (113) | + (115) | + (115) | + (101) | +/− (101) | Complex (108) |
| BM2A9 | − (103) | − (119) | + (92) | + (92) | + (99) | + (99) | Complex (92) |
| BM2B8 | − (95) | − (84 | + (88) | + (88) | + (109) | − (109) | Complex (81) |
| BM2B12 | − (118) | − (119) | + (109) | + (109) | + (109) | − (109) | Complex (108) |
| BM2A4 | − (111) | − (114) | NR | NR | − (89) | − (89) | Complex Unstable (103) |
| BMhTERT-2 mass culture | − (100) | − (96) | + (93) | + (93) | + (105) | + (105) | Complex (90) |

NOTE: Numbers in brackets indicate the population doublings at the time the assay was done.
Abbreviations: ND, not determined; NR, unable to amplify DNA by PCR.
*TP53 function determined by immunoblot analysis for p53 and p21$^{Cip1}$ following treatment with VP-16.
†Regulation of pRB determined by immunoblot analysis of phosphorylated and hypophosphorylated pRB following treatment with VP-16. +, normal hypophosphorylation response; −, no apparent response; +/−, partial phosphorylation response.
‡A simple karyotype was characterized by a near-diploid chromosome number and two or less karyotypic abnormalities. A complex karyotype included five or more chromosomal aberrations. BM2A4 had an unstable karyotype that was characterized by high frequency of random aberrations and numerous non-clonal marker chromosomes.
§Expression of p16$^{INK4a}$ by immunoblot analysis of protein and RT-PCR for detection of mRNA. +, expressed; −, not expressed; +/−, very low level expression.
‖Analysis of p16$^{INK4a}$ methylation status by bisulfite treatment, followed by real-time analysis of melting temperatures, direct and clonal PCR sequence analysis of CpG islands. +, methylated; −, unmethylated.

and p21$^{Cip1}$ was elevated 6 hours after drug treatment. Expression of p21$^{Cip1}$ remained high for at least 24 hours. Induction of p53 and p21$^{Cip1}$ followed a similar pattern in both pre- and post-crisis mass cultures, as well as in 11 of 12 post-crisis clones. Sequence analysis of exons 2 to 11 of the *TP53* gene confirmed wild-type sequence in all clones with complex karyotypes (data not shown). BM2A4 was the only clone to show *TP53* dysfunction, as it expressed no steady state or induced p53 and p21$^{Cip1}$ proteins (Fig. 4*B*). There was also no p53 mRNA detected in this clone by reverse transcription-PCR (data not shown). Thus, *TP53* was transcriptionally silenced on the apparently structurally normal copies of chromosome 17 detected in this cell line (Fig. 2*C*). It was notable that the p53/p21$^{Cip1}$ pathway was only defective in BM2A4, as this was the clone that showed the highest degree of karyotypic complexity and overt chromosomal instability (Tables 1 and 2). Together, the data indicate that disruption of *TP53* function was an infrequent event during immortalization of BMhTERTs. Furthermore, these data indicate that *TP53* dysfunction was not necessary for the evolution of complex karyotypes, although it may have conferred more overt genomic instability in BM2A4.

## Discussion

Our results showing that complex karyotypes evolved exclusively in BMhTERT cultures that silenced p16$^{INK4a}$ provide compelling evidence that p16$^{INK4a}$ plays a role in the maintenance of genomic integrity. Complex karyotypes in BMhTERT cells seemed to be the consequence of telomere dysfunction, as dramatic telomere shortening, telomere associations, and dicentric chromosomes were detected in cells with complex karyotypes. The nonreciprocal translocations, large deletions, and chromosome losses that were detected in BMhTERT karyotypes are typical outcomes of BFB cycles and classic features of human carcinomas and premalignant conditions (7–10).

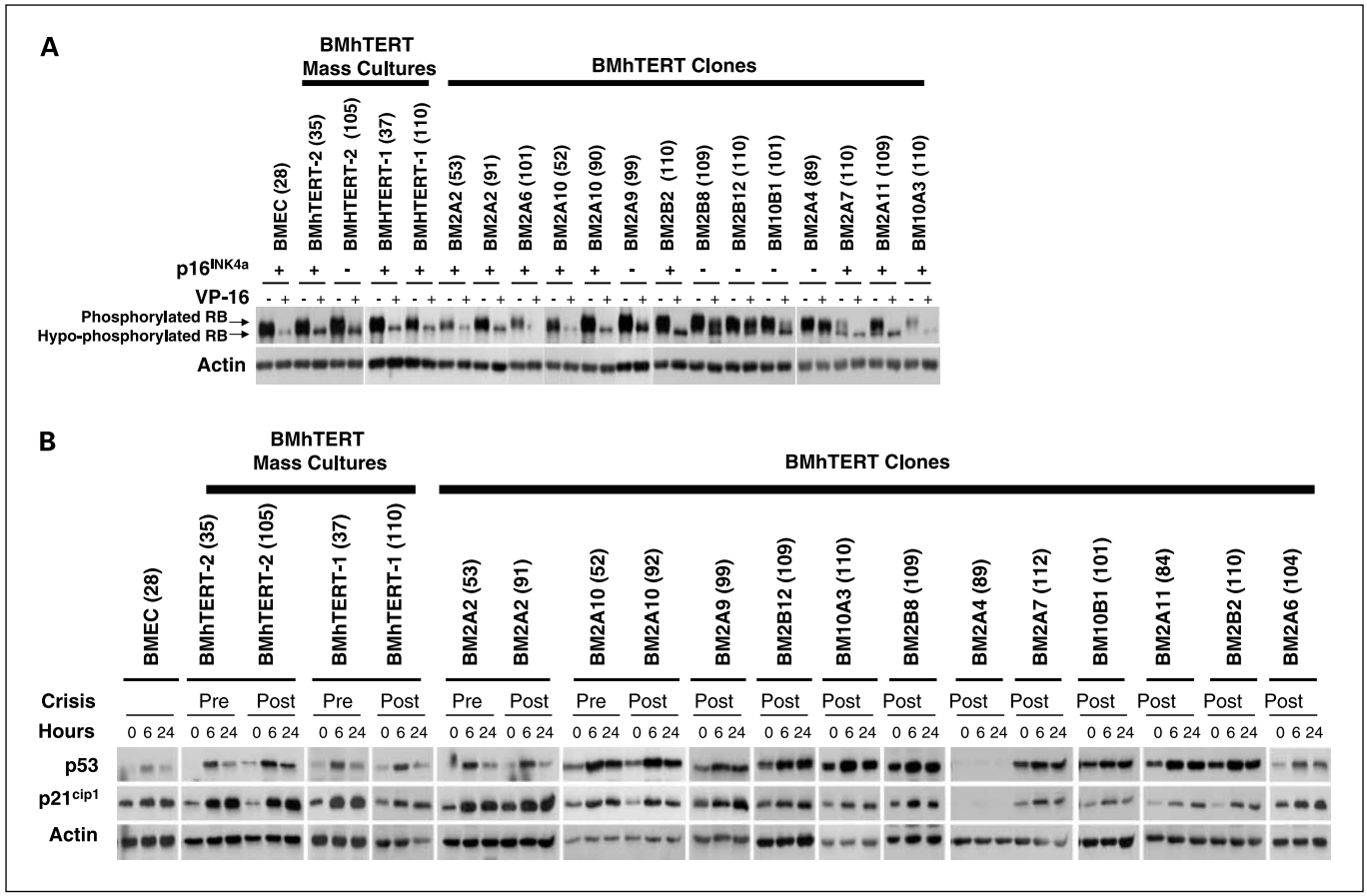


**Figure 4.** Phosphorylation of pRB and p53/p21$^{Cip1}$ protein expression in BMhTERT cells. *A,* immunoblot analysis of pRB in pre-crisis (35-53 population doublings) and post-crisis (89-110 population doublings) BMhTERT mass cultures and clones treated with 25 μmol/L VP-16 for 24 hours. Thick band demonstrates phosphorylated and hypophosphorylated pRB. The lower band is hypophosphorylated pRB. p16$^{INK4a}$ expression is indicated. *B,* immunoblot analysis of p53 and p21$^{Cip1}$ expression in VP-16-treated BMhTERTs at 6 and 24 hours. Numbers in brackets represent population doublings at the time the assay was done. *Pre,* pre-crisis (population doublings 35-53); *post,* post-crisis (population doublings 89-110).

It is well accepted that *TP53*-mediated DNA damage signals are elicited by telomere dysfunction. However, there is still considerable debate over whether telomere attrition also induces p16$^{INK4a}$, or if telomere-independent stresses, such as oxidative stress and culture stress, are responsible for induction of p16$^{INK4a}$ during senescence (16, 19). There are no prior reports of p16$^{INK4a}$ inactivation in human endothelial cells. However, previous studies have shown chromosomal aberrations and evidence of BFB cycles in mortal mammary epithelial cells that silenced p16$^{INK4a}$ by hypermethylation and proliferated beyond senescence (40, 41). However, in contrast to the immortalized endothelial cells described here, the epithelial cells in the latter studies did not express telomerase and eventually ceased proliferating. The most likely explanation for the correlation among p16$^{INK4a}$ repression, BFB events, and the evolution of complex karyotypes in BMhTERTs is that p16$^{INK4a}$ inactivation circumvented antiproliferative signals elicited by short telomeres and thereby enabled chromosomal abnormalities to accumulate. Because the *TP53* DNA damage pathway was defective in only one of six BMhTERT cell lines with complex karyotypes, our results are consistent with the possibility that p16$^{INK4a}$ is involved in *TP53*-independent antiproliferative effects elicited by telomere dysfunction (19). *TP53* dysfunction promotes chromosomal instability by enabling proliferation of premalignant cells with dysfunctional telomeres (5, 17). Our results suggest that repression of p16$^{INK4a}$ plays an analogous role in karyotypic evolution. Furthermore, our investigations show that a competent *TP53* DNA damage response pathway does not prevent telomere-driven karyotypic evolution. Nevertheless, *TP53* function did seem to confer some genetic stability in BMhTERTs, as the clone that expressed neither p16$^{INK4a}$ nor p53 displayed the most overtly unstable karyotype. The apparently additive effect of *TP53* dysfunction may reflect the role of *TP53* at both $G_1$ and $G_2$ cell cycle checkpoints, whereas p16$^{INK4a}$ is thought to function only at $G_1$ (18, 42).

Strikingly, many chromosome aberrations were common to different BMhTERT clones. Recurrent chromosome abnormalities occur in certain human cancers and were previously shown in association with telomere dysfunction in late-generation telomerase-negative mice (8). The recurrence of multiple chromosomal abnormalities may be attributed to an inherent susceptibility of the chromosomes with the shortest telomeres to form bridges and drive karyotypic evolution (43). The t(2;17)(p13;p13.3) translocation was the most frequent structural rearrangement detected in immortal BMhTERT cells (4 of 12 clones and 1 mass culture). Loss of subtelomeric DNA from chromosome arm 17p implicates telomere dysfunction in the generation of this abnormality. However, the single most common karyotypic alteration in BMhTERT cells was trisomy 11, which occurred in 9 of 12 clones

and 1 mass culture. Other frequent whole chromosome changes included loss of chromosomes 13 (6 of 12 clones) and Y (5 of 12 clones), as well as gains of chromosomes 19 (6 of 12 clones) and 20 (5 of 12 clones). Trisomy 11 and monosomy 13 frequently arise in cultures of normal endothelial cells and have an increased incidence in cultures approaching senescence (44, 45). However, it is unclear how BFB events would give rise to whole chromosome gains, such as +11, in the absence of other rearrangements. Furthermore, because no telomere fusions were detected in BMhTERT-1 cells, it seems likely that trisomy 11 was generated by an alternative mechanism.

The cytogenetic aberrations that were most frequently detected in post-crisis clones were not detected in 400 metaphase cells prepared from the BMhTERT-1 mass culture at early passage. However, we cannot rule out the possibility that these abnormalities were present at a very low frequency (<0.25%) and conferred a proliferative advantage or co-operated with hTERT in the immortalization process. Consistent with this possibility, many of the recurring aberrations have also been implicated in leukemia and carcinogenesis (46). For instance, trisomies 11 and 19 have been detected in myeloid leukemias. Monosomy 13 is indicative of a poor prognosis in multiple myeloma and is also observed in retinoblastoma and angiosarcoma (12, 46). Other abnormalities that angiosarcomas have in common with BMhTERT cells include cytogenetic complexity, aneuploidy, trisomies 20 and 11, loss of chromosome Y, and 17p deletions (12, 13). Thus, further characterization of genetic alterations in BMhTERT cells may provide insight to the molecular biology of these highly malignant endothelial cell–derived tumors, which remain poorly characterized due to their rarity. Subtelomeric deletion of 17p in association with t(2;17)(p13;p13.3) may have affected a number of putative tumor suppressor genes located at 17p13.3, such as *HIC1, OVCA1, OVCA2*, and *LOST1*, which are implicated in various human malignancies (46). Changes in gene copy number, resulting from the 17p rearrangement and other chromosomal aberrations, will be more precisely resolved in future studies by comparative genomic hybridization array analysis.

Our results, showing that p16$^{INK4a}$ was repressed in a subset (5 of 12) of immortal clones, and that the *TP53* pathway was dysfunctional in just one clone, indicate that defects in these pathways were not essential for immortalization of BMECs. Varied expression of p16$^{INK4a}$ was also noted when two hTERT-immortalized retinal pigmented epithelial clones were analyzed in a previous study (47). It is possible that these variations reflect clonal differences in p16$^{INK4a}$ expression in the parental cell strains. The growth crisis observed in 20 of 26 BMhTERT clones implicates additional molecular events in hTERT-mediated immortalization of BMECs. Time course of the BM10B1 cell line showed that crisis was unrelated to p16$^{INK4a}$ and *TP53* status. Crisis also did not seem to be related to specific cytogenetic aberrations or telomere length. The molecular events involved in crisis in BMhTERTs, therefore, remain to be determined. Clonal variations in the timing of crisis resulted in a masking effect in the BMhTERT-1 mass culture, which did not show a clear crisis. Similarly, we have previously shown proliferative variability among clones derived from a mass culture of hTERT-transduced MRC5 lung fibroblasts (30). Clonal variations, such as these, may contribute to some of the discordance among independent investigations into the effects of hTERT in various types of human cells.

The lack of mean telomere lengthening in BMhTERT cells was not due to low levels of telomerase activity, as the same hTERT vector induced very effective telomere lengthening in MRC5 lung fibroblasts (48). Furthermore, quantitation by real-time PCR showed that telomerase activity in BMhTERT clones was comparable with a number of tumor cell lines (additional data not shown). One likely explanation for shortening of mean telomere length in BMhTERTs is that oxidative stress overrode the lengthening capacity of telomerase (49). Mounting evidence indicates that the length of a subset of the shortest telomeres, rather than the average length of the telomeres, predicts proliferative arrest (50). Previous studies also suggest that telomerase may preferentially maintain the shortest telomeres (37, 38). The possibility that the subsenescent average telomere length of immortal BMhTERTs reflects selective maintenance of short telomeres is consistent with the eventual stabilization of average telomere length at ~3 kbp. Skewed densitometric TRF profiles of late-passage cells, which showed accumulation of shorter telomeres (data not shown), were also consistent with preferential maintenance of critically short telomeres. However, the telomere associations and consequential chromosomal rearrangements observed in the BMhTERT cells indicate that there was inadequate maintenance of at least a subset of telomeres at some stage of the immortalization process.

Taken together, the data from these investigations show that telomerase does not prevent telomere dysfunction during hTERT-mediated immortalization of BMECs. Moreover, these results show a specific association between p16$^{INK4a}$ inactivation and the evolution of karyotypic complexity in *TP53*-competent cells. These results suggest that p16$^{INK4a}$ may function as a gatekeeper to prevent telomere-driven cytogenetic evolution and provide a valuable model of the early stages of malignant transformation.

## Acknowledgments

Received 3/15/2006; revised 7/11/2006; accepted 9/14/2006.

**Grant support:** Cancer Institute of New South Wales (V.W. Wen and K.L. MacKenzie), New South Wales Cancer Council (V.W. Wen and K.L. MacKenzie), and National Health and Medical Research grant 293810 (R.A. Hinshelwood and S.J. Clark).

The costs of publication of this article were defrayed in part by the payment of page charges. This article must therefore be hereby marked *advertisement* in accordance with 18 U.S.C. Section 1734 solely to indicate this fact.

We thank Dale Wright (Sydney Genetics, Sydney IVF) for extensive consultation on cytogenetics and for reading this article.

## References

1. Chang E, Harley CB. Telomere length and replicative aging in human vascular tissues. Proc Natl Acad Sci U S A 1995;92:11190–4.
2. Moyzis RK, Buckingham JM, Cram LS, et al. A highly conserved repetitive DNA sequence, (TTAGGG)n, present at the telomeres of human chromosomes. Proc Natl Acad Sci U S A 1988;85:6622–26.
3. Griffith JD, Comeau L, Rosenfield S, et al. Mammalian telomeres end in a large duplex loop. Cell 1999;97:503–14.
4. Counter CM, Avilion AA, LeFeuvre CE, et al. Telomere shortening associated with chromosome instability is arrested in immortal cells which express telomerase activity. EMBO J 1992;11:1921–29.
5. Artandi SE, Chang S, Lee SL, et al. Telomere dysfunction promotes non-reciprocal translocations and epithelial cancers in mice. Nature 2000;406:641–5.
6. Hande MP, Samper E, Lansdorp P, Blasco MA. Telomere length dynamics and chromosomal instability in cells derived from telomerase null mice. J Cell Biol 1999;144:589–601.
7. Rudolph KL, Millard M, Bosenberg MW, DePinho RA. Telomere dysfunction and evolution of intestinal carcinoma in mice and humans. Nat Genet 2001;28:155–9.
8. O'Hagan RC, Chang S, Maser RS, et al. Telomere dysfunction provokes regional amplification and deletion in cancer genomes. Cancer Cell 2002;2:149–55.

**9.** O'Sullivan JN, Bronner MP, Brentnall TA, et al. Chromosomal instability in ulcerative colitis is related to telomere shortening. Nat Genet 2002;32:280–4.

**10.** Chin K, de Solorzano CO, Knowles D, et al. *In situ* analyses of genome instability in breast cancer. Nat Genet 2004;36:984–8.

**11.** Bell CD. Endothelial cell tumors. Microsc Res Tech 2003;60:165–70.

**12.** Schuborg C, Mertens F, Rydholm A, et al. Cytogenetic analysis of four angiosarcomas from deep and superficial soft tissue. Cancer Genet Cytogenet 1998;100:52–6.

**13.** Wong KF, So CC, Wong N, et al. Sinonasal angiosarcoma with marrow involvement at presentation mimicking malignant lymphoma: cytogenetic analysis using multiple techniques. Cancer Genet Cytogenet 2001;129:64–8.

**14.** Karlseder J, Broccoli D, Dai Y, Hardy S, de Lange T. p53- and ATM-dependent apoptosis induced by telomeres lacking TRF2. Science 1999;283:1321–5.

**15.** d'Adda di Fagagna F, Reaper PM, Clay-Farrace L, et al. A DNA damage checkpoint response in telomere-initiated senescence. Nature 2003;426:194–8.

**16.** Herbig U, Jobling WA, Chen BP, Chen DJ, Sedivy JM. Telomere shortening triggers senescence of human cells through a pathway involving ATM, p53, and p21(CIP1), but not p16(INK4a). Mol Cell 2004;14:501–13.

**17.** Chin L, Artandi SE, Shen Q, et al. p53 deficiency rescues the adverse effects of telomere loss and cooperates with telomere dysfunction to accelerate carcinogenesis. Cell 1999;97:527–38.

**18.** Ben-Porath I, Weinberg RA. The signals and pathways activating cellular senescence. Int J Biochem Cell Biol 2005;37:961–76.

**19.** Jacobs JJ, de Lange T. Significant role for p16INK4a in p53-independent telomere-directed senescence. Curr Biol 2004;14:2302–8.

**20.** Gimbrone MA, Jr., Fareed GC. Transformation of cultured human vascular endothelium by SV40 DNA. Cell 1976;9:685–93.

**21.** Fontijn R, Hop C, Brinkman H-J, et al. Maintenance of vascular endothelial cell-specific properties after immortalization with an amphotrophic replication-deficient retrovirus containing human papilloma virus 16 E6/E7 DNA. Exp Cell Res 1995;216:199–207.

**22.** Girardi AJ, Jensen FC, Koprowski H. SV40-induced transformation of human diploid cells: crisis and recovery. J Cell Comp Physiol 1965;65:69–84.

**23.** Kim NW, Piatyszek MA, Prowse KR, et al. Specific association of human telomerase activity with immortal cells and cancer. Science 1994;266:2011–4.

**24.** Bodnar AG, Oullette M, Froklis M, et al. Extension of life-span by introduction of telomerase into normal human cells. Science 1998;279:349–52.

**25.** Kiyono T, Foster SA, Koop JI, et al. Both Rb/p16INK4a inactivation and telomerase activity are required to immortalize human epithelial cells. Nature 1998;396:84–8.

**26.** Dickson MA, Hahn WC, Ino Y, et al. Human keratinocytes that express hTERT and also bypass a p16INK4a-enforced mechanism that limits lifespan become immortal yet retain normal growth and differentiation characteristics. Mol Cell Biol 2000;20:1436–47.

**27.** Tsutsui T, Kumakura S, Yamamoto A, et al. Association of p16(INK4a) and pRb inactivation with immortalization of human cells. Carcinogenesis 2002;23:2111–7.

**28.** Milyavsky M, Shats I, Erez N, et al. Prolonged culture of telomerase-immortalized human fibroblasts leads to a premalignant phenotype. Cancer Res 2003;63:7147–57.

**29.** Noble JR, Zhong ZH, Neumann AA, et al. Alterations in the p16(INK4a) and p53 tumor suppressor genes of hTERT-immortalized human fibroblasts. Oncogene 2004;23:3116–21.

**30.** Taylor LM, James A, Schuller CE, et al. Inactivation of p16INK4a, with retention of pRB and p53/p21cip1 function, in human MRC5 fibroblasts that overcome a telomere-independent crisis during immortalization. J Biol Chem 2004;279:43634–45.

**31.** Yang J, Chang E, Cherry AM, et al. Human endothelial cell lifespan extension by telomerase expression. J Biol Chem 1999;274:26141–8.

**32.** MacKenzie KL, Franco S, Naiyer AJ, et al. Multiple stages of malignant transformation of human endothelial cells modelled by co-expression of telomerase reverse transcriptase, SV40 T antigen and oncogenic N-ras. Oncogene 2002;21:4200–11.

**33.** O'Hare MJ, Bond J, Clarke C, et al. Conditional immortalization of freshly isolated human mammary fibroblasts and endothelial cells. Proc Natl Acad Sci U S A 2001;98:646–51.

**34.** Dai C, Krantz SB. Increased expression of the INK4a/ARF locus in polycythemia vera. Blood 2001;97:3424–32.

**35.** Huschtscha LI, Noble JR, Neumann AA, et al. Loss of P16(INK4) expression by methylation is associated with lifespan extension of human mammary epithelial cells. Cancer Res 1998;58:3508–12.

**36.** Clark SJ, Harrison J, Paul CL, Frommer M. High sensitivity mapping of methylated cytosines. Nucleic Acids Res 1994;22:2990–7.

**37.** Ouellette MM, Liao M, Herbet BS, et al. Subsenescent telomere lengths in fibroblasts immortalized by limiting amounts of telomerase. J Biol Chem 2000;275:10072–6.

**38.** Liu Y, Kha H, Ungrin M, Robinson MO, Harrington L. Preferential maintenance of critically short telomeres in mammalian cells heterozygous for mTert. Proc Natl Acad Sci U S A 2002;99:3597–602.

**39.** Gisselsson D, Pettersson L, Hoglund M, et al. Chromosomal breakage-fusion-bridge events cause genetic intratumor heterogeneity. Proc Natl Acad Sci U S A 2000;97:5357–62.

**40.** Romanov SR, Kozakiewicz BK, Holst CR, et al. Normal human mammary epithelial cells spontaneously escape senescence and acquire genomic changes. Nature 2001;409:633–7.

**41.** Soler D, Genesca A, Arnedo G, Egozcue J, Tusell L. Telomere dysfunction drives chromosomal instability in human mammary epithelial cells. Genes Chromosomes Cancer 2005;44:339–50.

**42.** Fukasawa K, Choi T, Kuriyama R, Rulong S, Vande Woude GF. Abnormal centrosome amplification in the absence of p53. Science 1996;271:1744–7.

**43.** der-Sarkissian H, Bacchetti S, Cazes L, Londono-Vallejo JA. The shortest telomeres drive karyotype evolution in transformed cells. Oncogene 2004;23:1221–8.

**44.** Johnson TE, Umbenhauer DR, Hill R, et al. Karyotypic and phenotypic changes during *in vitro* aging of human endothelial cells. J Cell Physiol 1992;150:17–27.

**45.** Zhang L, Aviv H, Gardner JP, et al. Loss of chromosome 13 in cultured human vascular endothelial cells. Exp Cell Res 2000;260:357–64.

**46.** Dessen P, Knuutila S, Huret JL. Chromosome 17. Atlas of Genetics and Cytogenetics in Oncology and Haematology [homepage on the Internet]. 2002 [updated 2006 Aug 28; cited 2006 Aug 28] Available from: http://AtlasGeneticsOncology.org/Indexbychromosom/idxa_17.html.

**47.** Jiang XR, Jimenez G, Chang E, et al. Telomerase expression in human somatic cells does not induce changes associated with a transformed phenotype. Nat Genet 1999;21:111–4.

**48.** MacKenzie KL, Franco S, May C, Sadelain M, Moore MAS. Mass cultured human fibroblasts overexpressing hTERT encounter a growth crisis following an extended period of proliferation. Exp Cell Res 2000;259:336–50.

**49.** Kurz DJ, Decary S, Hong Y, et al. Chronic oxidative stress compromises telomere integrity and accelerates the onset of senescence in human endothelial cells. J Cell Sci 2004;117:2417–26.

**50.** Hemann MT, Strong MA, Hao LY, Greider CW. The shortest telomere, not average telomere length, is critical for cell viability and chromosome stability. Cell 2001;107:67–77.